

Carbonate content and stable isotopic composition of atmospheric aerosol carbon in the Canadian High Arctic

Petr Vodička^{1,2}, Kimitaka Kawamura², Bhagawati Kunwar^{2,3}, Lin Huang⁴, Dhananjay Kumar^{2,a}, Md. Mozammel Haque^{2,5}, Ambarish Pokhrel², Sangeeta Sharma⁴, Leonard Barrie⁶

¹ Institute of Chemical Process Fundamentals, Czech Academy of Sciences, 165 00 Prague 6, Czech Republic

² Chubu Institute for Advanced Studies, Chubu University, 1200 Matsumoto-cho, Kasugai 487–8501, Japan

³ Institute for Space-Earth Environmental Research, Nagoya University, Nagoya 464-8601, Japan

⁴ Environment and Climate Change Canada, Science and Technology Branch, 4905 Dufferin St., Toronto, Canada

⁵ School of Ecology and Applied Meteorology, NUIST, Nanjing, 210044, China

⁶ Atmospheric and Oceanic Sciences Department, McGill University, Montreal, Canada

^a Now at: Commission for Air Quality Management in National Capital Region and Adjoining Areas, New Delhi 110001, India

Correspondence to: Petr Vodička (vodicka@icpf.cas.cz) and Kimitaka Kawamura (kkawamura@isc.chubu.ac.jp)

Abstract. The carbon cycle in the Arctic atmosphere is important in understanding abrupt climate changes occurring in this region. Two-years of measurements (summer 2016 - spring 2018) of carbonaceous aerosols at the High Arctic station Alert, Canada, showed that in addition to organic carbon (OC) and elemental carbon (EC), carbonate carbon (CC) was episodically but not negligibly present. The relative abundances of CC in total carbon (TC) ranged from 0–65 % with an average of approximately 11 % over the entire period. Also there was a strong correlation of CC with aerosol Ca²⁺ which is associated mostly with soil dust and to a lesser extent sea salt aerosol. Based on this and the analysis of air mass back trajectories (AMBT), we infer two possible sources of CC in the Arctic total suspended particles (TSP). The major one is the erosion and resuspension of limestone sediments, particularly in the semi-desert areas of the northern Canadian Arctic. Another potential minor source of CC is marine aerosol including calcified marine phytoplankton shells (coccoliths) introduced into the atmosphere via sea-to-air emission.

The CC content significantly influenced the stable carbon isotopic composition ($\delta^{13}\text{C}$) of TC. The higher the CC content, the higher the $\delta^{13}\text{C}$ values, which is consistent with the strong ¹³C enrichment in carbonates. Therefore, carbonates in Arctic TSP must be taken into account not only in isotopic studies using $\delta^{13}\text{C}$ analyses but also when assessing the impact of carbonaceous aerosols on the Arctic climate.

Deleted: . Deshmukh

Deleted: more

Deleted: from

Deleted: sources

Deleted:

1 Introduction

The Arctic is a dynamically changing region that is significantly affected by climate change (England et al., 2021). Aerosols are one of the factors influencing the climate, but their effects are subject to significant uncertainties (Carslaw et al., 2013). The uncertainties in radiative forcing is primarily associated with carbonaceous aerosols, most of which is composed of organic carbon (OC). In contrast, a smaller fraction consists of elemental carbon (EC), which is equivalent to optically determined black carbon (BC) (Petzold et al., 2013).

Organic aerosols, i.e., OC in the atmosphere, generally have a cooling effect on the climate (Stjern et al., 2016) except for the part called brown carbon (Laskin et al., 2015). On the other hand, EC or BC has the warming effect, both in the atmosphere (Liu et al., 2020) and on snow surface (Flanner et al., 2007) especially important in the Arctic. In addition, EC and BC measurements are also used to determine the mass absorption cross section (MAC), a fundamental input to radiative transfer models (Mbengue et al., 2021). The MAC is season- and station- specific (Savadkoobi et al., 2024), making it one of the parameters in affecting the influence of aerosols on climate. If either EC or BC is determined inaccurately, the MAC factor will be subsequently biased as well (Chen et al., 2021). Therefore, detailed knowledge of the composition of carbonaceous aerosol in the Arctic is crucial for improving our understanding of their impacts on the climate changes in this region.

Recent atmospheric studies from Tajikistan (Chen et al., 2021) and Tibet (Hu et al., 2023) indicate a significant contribution of carbonates in total suspended particles (TSP), which may have a significant effect on the determination of OC and EC (or BC). Those areas are characterized as arid desert regions with sparse vegetation, large amounts of unconsolidated sediments, and lack of soil moisture, where the wind erosion plays an important role in the aeolian processes such as atmospheric transports and dust deposits. Arctic regions are affected by long range transport of dust and also contributed by dust locally (Groot Zwaafink et al., 2016; Sharma et al., 2019; Sirois and Barrie, 1999). They have a desert, semi-desert or arid character in some cases (Pushkareva et al., 2016). Recently high-latitude dust sources have been described as a significant climate and environmental factor (Kawai et al., 2023; Kawamura et al., 1996; Meinander et al., 2022). It is reported that carbonate rich dust also has a slightly positive effect on radiative forcing, although lower than BC (Chen et al., 2021; Raman et al., 2011). High Arctic semi-desert aerosols have been described as potentially important reservoirs of soil organic matter (Muller et al., 2022), however, the influence of carbonates on the atmosphere in these regions has not yet been systematically studied. Investigation of the ion balance of November to May fresh snowfall at Arctic site Alert over a three year period (Toom-Sauntry and Barrie, 2002) led to the conclusion that missing carbonate (especially in November and May) is the most likely cause of the ion imbalance. In addition to dust, it is hypothesized

that a source of carbonates in summer Arctic aerosols may be marine microorganisms from sea spray as reported by Mukherjee et al. (2020) based on calcium analyses.

In recent years, carbon in aerosols has also been subject to analyses of the stable isotopic composition ($\delta^{13}\text{C}$) as a method for studying atmospheric processes (Gensch et al., 2014; Huang et al., 2006). Several studies within the Arctic have also employed $\delta^{13}\text{C}$ analysis to study carbonaceous aerosols. Specifically, at the Canadian Alert station, studies investigating $\delta^{13}\text{C}$ changes in the EC (Rodríguez et al., 2020; Winiger et al., 2019) and springtime $\delta^{13}\text{C}$ changes in the TC (Narukawa et al., 2008) have recently been published.

Carbonates are strongly enriched in ^{13}C , with relatively positive $\delta^{13}\text{C}$ around zero, and can thus affect $\delta^{13}\text{C}$ values in TC of TSP aerosols, as demonstrated by Chen et al. (2016) for Asian desert dust. In the Arctic region, observed higher aerosol $\delta^{13}\text{C}$ values in atmospheric aerosols are often attributed to dissolved particulate organic matter from marine aerosol sources while the influence of carbonates is ignored (Gu et al., 2023). We hypothesized that the influence of carbonates on Arctic aerosols is not negligible. In this study, we present two years of carbonaceous aerosol observations at the Alert focusing on carbonate content and the isotopic composition of $\delta^{13}\text{C}$ of TC.

Deleted: are

2 Experimental

2.1 Measurement site and sampling

TSP samples were collected at the WMO Global Atmosphere Watch Observatory at Alert, Nunavut, Canada ($82^{\circ}27'03.0''\text{ N}$, $62^{\circ}30'26.0''\text{ W}$, 210 m ASL). The Alert site represents a remote Arctic area located on the northeastern tip of Ellesmere Island, which is 817 km from the North Pole (Fig. 1). The site has been used for research on atmospheric aerosols since the mid-1980s (Barrie and Barrie, 1990). In terms of carbonaceous aerosols, BC has been measured at the station for decades (Sharma et al., 2004, 2017). Rodríguez et al. (2020) later then reported EC/OC results from TSP between March 2014 to June 2015 with a focus on EC analyses.

For this study, TSP samples were collected from June 13, 2016 to April 16, 2018, using a high-volume sampler on pre-baked (450°C , 12 h) quartz fiber filters (20 x 25 cm, PALL, 2500QAT-UP). During this period, a total of 93 samples were collected at weekly intervals. The sampled filters were placed in clean glass jars with Teflon-lined caps and stored in a freezer before chemical analyses.



Figure 1. Map of the site position (asterisk) and geographical boundaries for dominant source regions of backward air mass trajectories (Arctic Ocean - blue, Greenland - green, North Canada islands - red, North America - purple, Siberia - grey, and Europe - yellow). Background map by Wikimedia Commons / Public Domain.

2.2 Analyses

To obtain the TSP mass concentration, each filter was weighed before and after sampling, and resulting concentrations were corrected for the corresponding field blank filter. Subsequently, we analyzed the samples by two methods to measure the carbonaceous components, with the outputs shown in **Fig. 2**.

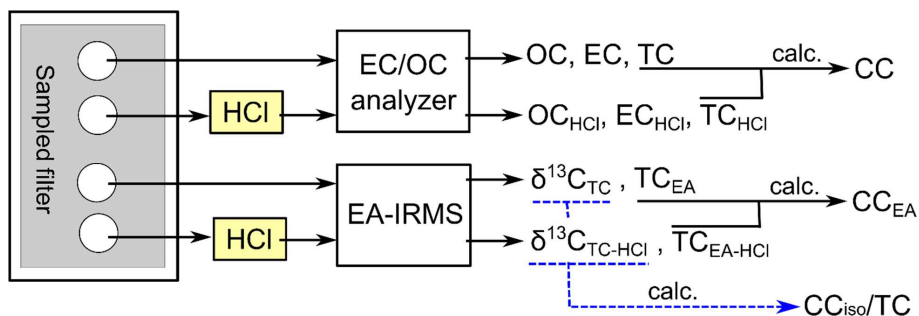


Figure 2. Diagram showing the method for the measurements of carbonaceous components in quartz fiber filter samples.

Contents of OC, EC and total carbon (TC) were determined using a Sunset semi-continuous analyzer (Sunset Laboratory Inc., Tigard, OR, USA; (Bauer et al., 2009)) operated in off-line mode. Samples with a diameter of 16 mm (area 2.01 cm²) were analyzed by Improve_A temperature protocol: step [gas] temperature (°C)/duration (s): helium (He) 140/120, He 280/120, He 480/120, He 580/120, He-O₂ (Ox.) 580/120, He-O₂ 740/120, He-O₂ 840/210 (Chow et al., 2007). Split point between OC and EC was determined based on laser beam (660 nm) transmittance measurements through the filter during analysis and raw data were subsequently evaluated by RTCalc726 software (Sunset Lab). The same EC/OC analysis was performed after exposing the aerosol filters to HCl vapors overnight in a desiccator. From the difference of TC and TC_{HCl}, the content of CC was calculated, which is discussed further in subsection 2.3.

The same samples were further analyzed for the stable carbon isotopic composition ($\delta^{13}\text{C}$) of TC by the method described in more detail elsewhere (Vodička et al., 2022). Briefly, filter cuts (2.01 cm²) were placed in tin cups, inserted into the elemental analyzer (EA, Flash 2000) and heated to 1000 °C in a helium atmosphere. At this temperature, carbonaceous compounds are evolved and catalytically oxidized to CO₂, which was isolated on a packed gas chromatograph, and then measured for TC by a thermal conductivity detector, and finally transferred into the isotope ratio mass spectrometer (IRMS; Delta V, Thermo Fischer Scientific) via a ConFlo IV interface for the analyses of ¹³C/¹²C ratios. An external standard, acetanilide (supplied by Thermo Electron Corp.), having a $\delta^{13}\text{C}$ of -27.26 ‰ compared to Vienna Pee Dee Belemnite (VPDB), was used to obtain calibration curves for total carbon (TC) and its isotopic values. Subsequently, we determined the $\delta^{13}\text{C}$ of TC using Eq. (1) with relation to the international standard VPDB.

$$\delta^{13}\text{C} (\text{‰}) = [({}^{13}\text{C}/{}^{12}\text{C})_{\text{sample}} / ({}^{13}\text{C}/{}^{12}\text{C})_{\text{standard}} - 1] \times 10^3 \quad (1)$$

136 In this manner, $\delta^{13}\text{C}_{\text{TC}}$, corresponding to delta TC values on the filter, and $\delta^{13}\text{C}_{\text{TC-HCl}}$, representing delta
137 values on filters after exposure to HCl vapor, were analyzed. The standard deviation of $\delta^{13}\text{C}$ measurements
138 based on triplicate sample analysis was 0.03 ‰.

139 Through these analyses, we obtained TC from two independent analytical techniques. We observed good
140 agreement between TC value measured by the EC/OC analyzer and those by EA ($r = 0.98$). We also
141 obtained a good agreement even after HCl treatment of the filters ($r = 0.98$) (**Fig. S1**). The slightly higher
142 TC concentrations using EA (2 ‰) may be due to the use of a higher maximum temperature (1000 °C vs
143 840 °C) for sample release.

Deleted: 9

145 2.3 Characteristics of carbonate carbon (CC)

146 Concentrations of CC, one of the key variables of this study, were calculated from the difference of TC
147 before and after HCl fumigation (**Eq. (2)**)

$$148 \text{CC} = \text{TC} - \text{TC}_{\text{HCl}} \quad (2)$$

149 **Eq. (2)** defines CC, or nominal CC. This procedure is probably not able to analyze all carbonates (Baudin
150 et al., 2023) but quantitatively, this method leads to the analysis of at least 90% of the carbonates in samples
151 (Karanasiou et al., 2011). **Fig. 3** shows thermograms from OC-EC analyses of a selected sample without
152 HCl treatment (purple curve) and after HCl treatment (green curve). As shown in **Fig. 3**, the largest material
153 loss can be seen at the temperature step EC2, but for other samples we observed the largest material losses
154 in the EC1 and OC4 regions as well. These are temperature steps during which we should expect the release
155 of carbonate carbon (CC) (Cavalli et al., 2010; Chow et al., 1993). On the other hand, removal of carboxylic
156 acids (e.g. acetic or oxalic acid) can be expected at temperature steps OC2 and OC3 (Hasegawa, 2022).
157 Exposing samples to HCl can also affect the transformation of organic matter, which is then released at
158 higher temperatures. Therefore, the thermogram after fumigation may not reflect only the expected CC loss
159 (Jankowski et al., 2008). We also analyzed several carbonate and oxalate salt standards as a control (**Fig.**
160 **S2**). The thermogram of the sample with a pronounced peak in the EC2 region (**Fig. 3**) was most similar to
161 that of CaCO_3 (**Fig. S2a**). Hence, it can be assumed that the significant peaks, removed by HCl in the EC2
162 region of thermogram, are carbonate in origin. Nevertheless, it cannot be excluded that some of the
163 prominent CC peaks in the OC4 region are also from oxalates as confirmed also by additional analyses of
164 CaCO_3 and potassium oxalate monohydrate standards before and after HCl fumigation (**Fig. S2b**). The
165 nominal CC may contain other minor carbon components. Here, however, it should also be noted that the

167 reported values of oxalates in the Arctic (see, e.g., Feltracco et al. (2021), Svalbard) are an order of
168 magnitude lower than the CC values we analyzed.

169 It is worth noting here that if we did not analyze CC, it would be determined as either OC or EC based on
170 the thermogram and automatic determination of the split point (Fig. 3). For both EC and OC, we calculated
171 the percentage of mass removed by HCl fumes as CC using an Eqs. (3) and (4).

172
$$EC_{\text{removed}} (\%) = (EC - EC_{\text{HCl}}) / EC * 100 \quad (3)$$

173
$$OC_{\text{removed}} (\%) = (OC - OC_{\text{HCl}}) / OC * 100 \quad (4)$$

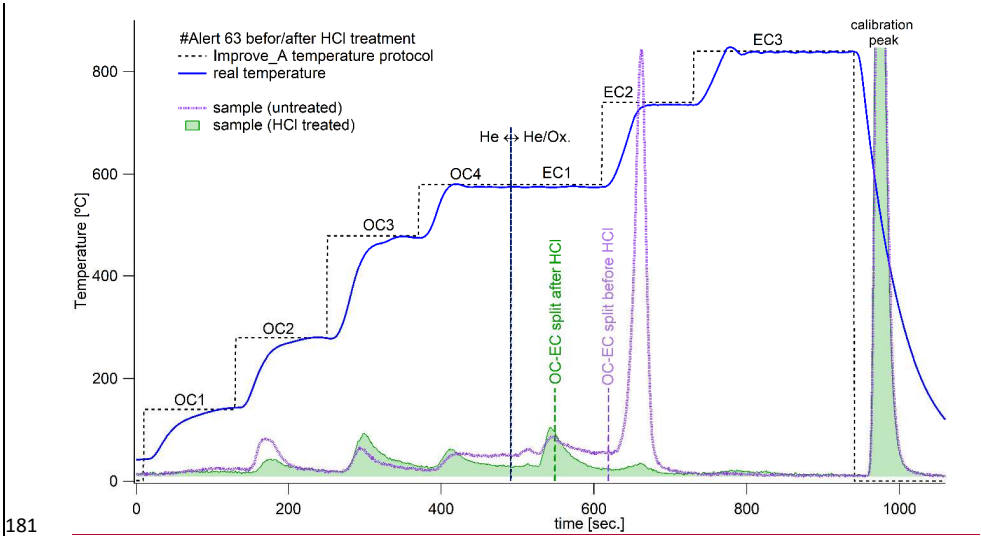
174 In this way, we found that the CC contribution was, on average, 25 % (ranging from 0 to 81%) of EC and
175 12 % (ranging from 0 to 46 %) of OC which have been inaccurately determined if we had not assessed the
176 CC contribution. On a relative basis, EC concentrations were more biased in all seasons (Fig. S3).

177 Analyses for CC were performed by two independent methods (EC/OC and EA instruments, Fig. 2), and
178 the resulting CC values show acceptable agreement (Fig. S4). Fig. S4 shows that CC values based on
179 analyses from the EC/OC analyzer may be slightly underestimated. However, unless otherwise stated, CC
180 values calculated from EC/OC analyses are discussed in this study.

Deleted: good

Deleted: $r = 0.87, y = 0.95 x,$

Deleted: U



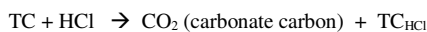
182 **Figure 3.** Example of EC/OC analysis of untreated (purple thermogram) and treated sample with HCl
183 fumigation (green thermogram) by Improve A temperature protocol. The vertical black dashed line shows

Deleted: .

a change in the use of He and the He/Ox. mixture in the analysis. The green and purple vertical dashed lines show the automatic determination of split point between OC and EC. Sample #Alert-63 was collected from 15-22 May 2017.

2.4 Estimate of $\delta^{13}\text{C}$ values of CC

The $\delta^{13}\text{C}$ analyses of TC and TC_{HCl} allowed us to estimate $\delta^{13}\text{C}$ of CC. Here we calculate the $\delta^{13}\text{C}$ values of released CC on HCl fumigation using the following reaction and the isotopic mass balance equation (Eq. 5), being similar with the calculation in Kawamura and Watanabe (2004).



$$\delta^{13}\text{C}_{\text{TC}} = f * \delta^{13}\text{C}_{\text{CC}} + (1-f) * \delta^{13}\text{C}_{\text{TC-HCl}} \quad (5)$$

, where f means a fraction of CC in TC. From Eq. 5, we derived the formula for calculating $\delta^{13}\text{C}_{\text{CC}}$ (Eq. 6).

$$\delta^{13}\text{C}_{\text{CC}} = (\delta^{13}\text{C}_{\text{TC}} - (1-f) * \delta^{13}\text{C}_{\text{TC-HCl}}) / f \quad (6)$$

The $\delta^{13}\text{C}_{\text{CC}}$ values were reasonable for a CC content in the TC of approximately above 20 % (Fig. S5). When f (CC contribution) is high, $\delta^{13}\text{C}_{\text{CC}}$ values are close to zero, supporting that CC is mainly composed of carbonate, such as CaCO_3 . However, when the f values are low, the $\delta^{13}\text{C}_{\text{CC}}$ are highly scattered, indicating that the released (removed) carbon by HCl is not only carbonate carbon but also contains various types of carbon including semi-volatile organic acids or unknown species. In the case of organic acids, $\delta^{13}\text{C}$ values can be as high as -10‰ (e.g., Wang and Kawamura, 2006) or positive due to unknown isotope fractionation during analytical processing. Highly scattered values may also be due to potential analytical errors in EA-IRMS measurements when f is sufficiently small. If the CC contribution were zero, Eq. 6 would lead to division by zero. This may also be the cause of bias and scattering of $\delta^{13}\text{C}_{\text{CC}}$ values at low CC contributions (Fig. S5).

2.5 Carbonate estimation from isotopic composition

We used the isotopic mass balance between $\delta^{13}\text{C}_{\text{TC}}$ and $\delta^{13}\text{C}_{\text{TC-HCl}}$ as an alternative and probably more accurate method to determine carbonate content (CC_{iso}) in TC. The $\text{CC}_{\text{iso}}/\text{TC}$ (f_{iso}) calculation is based on the assumption that the $\delta^{13}\text{C}$ of carbonates is around 0‰ with an approximate range $+5\text{‰}$ to -5‰ , and no other compounds are present in this range. We used Eq.5, where $\delta^{13}\text{C}_{\text{TC}}$ and $\delta^{13}\text{C}_{\text{TC-HCl}}$ are known and $\delta^{13}\text{C}_{\text{CC}}$ are given by three different values, covering an approximate range of carbonates ($+5\text{‰}$, 0‰ , -5‰).

217 While $\delta^{13}\text{C}_{\text{CC}} = 0$, $f = 1 - (\delta^{13}\text{C}_{\text{TC}} / \delta^{13}\text{C}_{\text{TC-HCl}})$ (7)

218 While $\delta^{13}\text{C}_{\text{CC}} = +5$, or -5 , $f = (\delta^{13}\text{C}_{\text{TC}} - \delta^{13}\text{C}_{\text{TC-HCl}}) / (\delta^{13}\text{C}_{\text{CC}} - \delta^{13}\text{C}_{\text{TC-HCl}})$ (8)

219 The f_{iso} value is then an average calculated from the three f values obtained from **Eqs. 7 and 8**.

220

221 **2.6 Auxiliary data**

222 Air mass back trajectories (AMBT) were calculated using the National Oceanic and Atmospheric
223 Administration (NOAA) HYSPLIT model (Stein et al., 2015) at 500 m a.g.l. using a run time 168 h in
224 GDAS (Global Data Assimilation System) with 0.5 degree resolution for each sampling days. For
225 subsequent analyses, we divided the air masses into six sectors as depicted in **Fig 1**.

226 Meteorological data at 5 min resolution for temperature (T), wind speed (WS) and wind direction (WD)
227 were provided by Environment and Climate Change Canada. Only WDs between 14 November 2016 and
228 16 January 2017 were obtained from the NOAA website (<https://psl.noaa.gov/arctic/observatories/alert/>).
229 For the purpose of this study, complementary mean values of T and WS were calculated to each sample.

230 The WD and WS data were used to create wind roses by Zefir software (Petit et al., 2017) and used in
231 combination with the AMBT data to determine the predominant aerosol origin for each sample. All wind
232 roses and AMBT by HYSPLIT are shown in supplementary data.

233 The water soluble ions (Ca^{2+} , Mg^{2+} , Na^{+}) were measured using an ion chromatography (761 Compact IC,
234 Metrohm, Switzerland). For this purpose, the filtered samples were twice extracted with 10 ml of ultrapure
235 water using an ultrasonic bath for 15 min and the aqueous extracts were filtered using a disc filter (Millex-
236 GV, 0.22 μm , Millipore).

237

238 **3 Results and discussion**

239 **3.1 Carbonaceous aerosol composition**

240 Time series of TC, OC_{HCl} , EC_{HCl} and CC mass concentrations are shown in **Fig. 4**. An overview of results
241 is provided for the seasonal variations from 2016 to 2018 in **Table 1** and **Fig. S6** in supplementary material.
242 An average TC concentration over the entire measurement period was $0.219 \pm 0.147 \mu\text{g m}^{-3}$ (median 0.186
243 $\mu\text{g m}^{-3}$; deviation due to one sample with a concentration of $1.22 \mu\text{g m}^{-3}$, **Fig. 4a**). Average TC contribution
244 in aerosol mass ranged from 5 to 14% (**Table 1**). Seasonally, the highest mass concentrations of TC, OC_{HCl}
245 and EC_{HCl} were found in winter and/or spring (**Fig. S6, Table 1**).

246 The fact that EC_{HCl} corresponds to realistic elemental carbon concentrations is demonstrated by comparison
247 with the study of Rodríguez et al. (2020), who analyzed EC in TSP during 2014-2015. They reported
248 seasonal EC concentrations that are similar to our observed EC_{HCl} , while their CC was part of the OC due
249 to the use of a different temperature protocol (EnCan-Total-900) during the OC/EC analysis. However,
250 Rodríguez et al. (2020) did not quantify the contribution of CC to TC.

251 Concentrations of OC_{HCl} dominate in all seasons (**Figs. 4b** and **5**) but present seasonally different
252 correlations with ambient temperature. Especially in summer, we observe a significant positive correlation
253 ($r = 0.73$) between OC_{HCl} concentrations and temperature (**Fig. S7a**). A similar relationship was also
254 observed, e.g., at the subarctic station Pallas (Friman et al., 2023), suggesting a biogenic origin of
255 summertime organic aerosols in Arctic areas (Moschos et al., 2022). In contrast, we observe negative
256 correlations between OC_{HCl} and ambient temperature in winter ($r = -0.15$, insignificant) and spring ($r = -$
257 0.43). A year-round similar trend for EC_{HCl} ($r = -0.39$, **Fig. S7b**), supporting previous studies that highlight,
258 in particular, the anthropogenic contributions to Arctic aerosol during the polar night (Moschos et al., 2022).
259 However, for CC, we observe no significant dependence on temperature ($r = 0.09$, **Fig. S7c**).

260

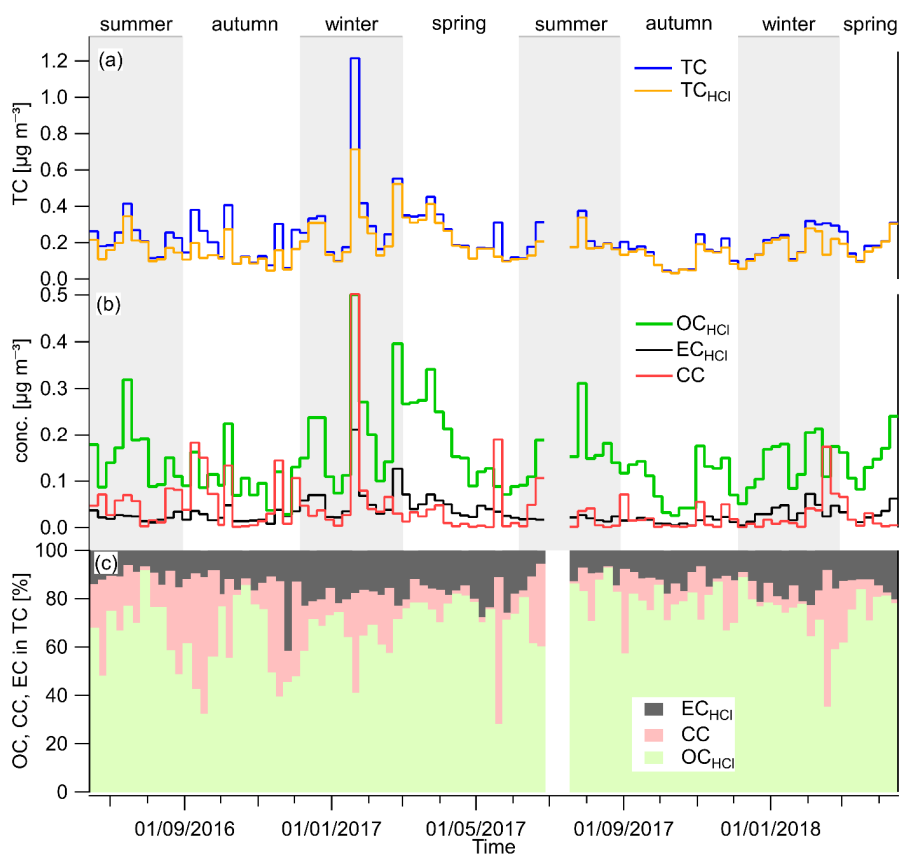
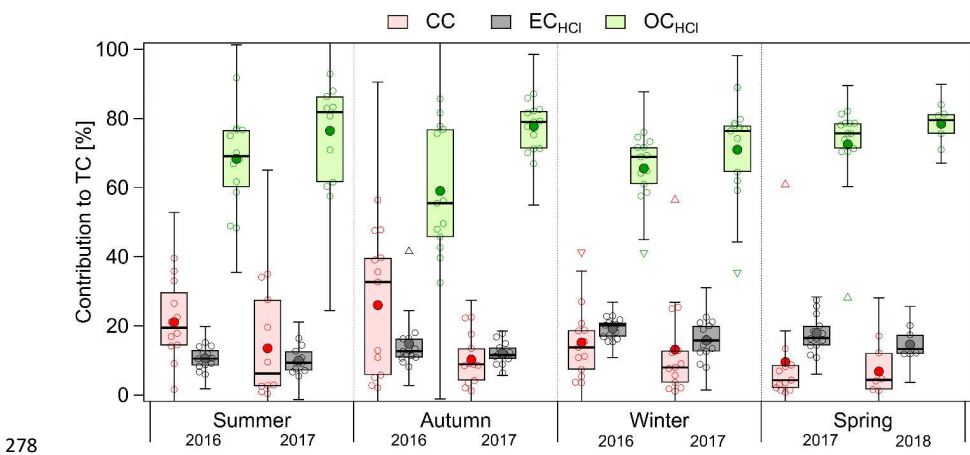


Figure 4. Time series of (a) TC mass concentrations before and after HCl treatment of samples, (b) OC, EC and CC mass concentrations, and (c) their relative contributions to TC in the Alert TSP aerosols.

Time series of TC before and after HCl fumigation (**Fig. 4a**) show that the amount of carbon removed in the form of CC is neither negligible nor large. However, both mass concentrations of CC (**Fig. 4b**) and its relative contributions (**Fig. 4c**) show that the CC is often larger than the EC_{HCl} contribution. Specifically, CC concentrations were highest during both autumn of 2016 and summer of 2016 and 2017 (**Fig. S6c**), which was reflected also in the relative contributions to TC (**Table1, Fig. 5**).

270 It is notable to understand the origin of CC. During summer, the contribution of biogenic aerosols (a
 271 potential source of oxalates) is highest, while the landscape is least covered by snow, making the situation
 272 favorable for resuspension of soils eroded from rocks including carbonates. A potential source of carbonates
 273 may come directly from the Canadian Arctic land region, where limestone sediments are reported to be
 274 abundantly present (Groot Zwaaftink et al., 2016; Not and Hillaire-Marcel, 2012; Phillips and Grantz, 2001).
 275 Another likely source of carbonate is marine aerosols as marine organisms contribute carbonate to the sea
 276 (Stein et al., 1994). In the context of wind directions and the effect on $\delta^{13}\text{C}$, the origin of CC is further
 277 discussed in the following subsection 3.2.



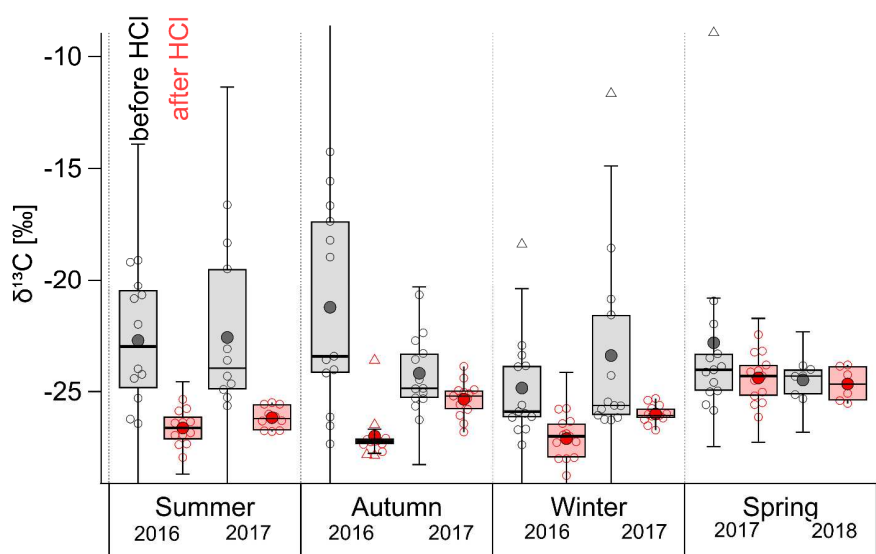
279 **Figure 5.** Seasonal contributions of CC, EC_{HCl} and OC_{HCl} to TC. The boxes correspond to the interquartile
 280 range (IQR; 25 and 75 percentile) with median represented by the inner solid line. The whiskers correspond
 281 to inner fences range (1.5*IQR), triangles are outliers and mean is represented by large filled circle.

282
 283 **3.2. Stable carbon isotopic composition**

284 Removal of CC by HCl fumigation has a significant effect on the measurements of $\delta^{13}\text{C}$ isotopic values of
 285 TC (**Figs. 6 and 7**). **Fig. 6** shows a seasonally resolved $\delta^{13}\text{C}$ values for HCl-treated (red) and untreated
 286 (grey) samples. We observed significant changes in all seasons except in spring of 2017 and 2018. Here it
 287 is interesting to mention a link with Narukawa et al. (2008), who reported changes in $\delta^{13}\text{C}$ of TC values for
 288 HCl-treated samples between winter and spring at Alert site. Narukawa et al. (2008) show significantly
 289 higher $\delta^{13}\text{C}$ values in spring than winter and related this to the possible contribution of carboxylic acids

(especially oxalic acid). During our observations, the differences in average values of $\delta^{13}\text{C}$ of TC (HCl treated vs. untreated) were also significant (see red boxes in **Fig. 6** and **Table 1**). Winter and spring $\delta^{13}\text{C}$ values after HCl treatment in this study (**Table 1**) are similar to those presented by Narukawa et al. (2008) for the year 2000. Thus, this study confirms that this is a long-term phenomenon likely to occur annually.

294



295

Figure 6. Seasonal variations of $\delta^{13}\text{C}$ of TC of untreated (grey) and HCl treated (red) TSP samples at Alert site from summer 2016 to spring 2018. The boxes correspond to the interquartile range (IQR; 25 and 75 percentile) with median represented by the inner solid line. The whiskers correspond to inner fences range ($1.5 \times \text{IQR}$), triangles are outliers and mean is represented by large filled circle.

300

In addition, measurements of $\delta^{13}\text{C}$ in OC, pyrolytic carbon (POC) + CC, and EC, performed at Environment Canada Toronto Laboratory, using ECT9 temperature protocol (Huang et al., 2006, 2021) for the fine particle (PM_{10}) samples collected around 2003, support that a noticeable fraction of CC occurs during the summer months, as indicated by the relatively more positive $\delta^{13}\text{C}$ of “POC+CC” fraction (**Fig. S8**).

Carbonate from eroded rocks in terrestrial environment usually generates large particles, so the CC content in PM_{10} should be lower than that in TSP. Consequently, the $\delta^{13}\text{C}$ TC in PM_{10} is expected to be relatively

Deleted: ip

308 less positive of compared to that that in TSP. Therefore, **Fig. S8** suggests that the impact of CC on $\delta^{13}\text{C}$ TC
309 is an annual phenomenon occurring over decadal periods. The tendency towards relatively more positive
310 $\delta^{13}\text{C}$ in summer OC fraction also suggests the presence of minor salt oxalate, or potassium or magnesium
311 carbonates, which are released at 550 °C or lower, as shown in **Fig. S2**. In the time series in **Fig. 7**, we
312 observed episodes with significant differences in $\delta^{13}\text{C}$ values and alternating over short periods. The
313 comparison of $\delta^{13}\text{C}$ of TC and TC mass concentration for both HCl untreated and treated samples shows
314 insignificant correlation (**Fig. S9**). However, we found a significant, though not strong, correlation of $\delta^{13}\text{C}$
315 with wind speed (**Fig. S10**) ($r = 0.36$) and a negative correlation after HCl fumigation ($r = -0.32$ for $\delta^{13}\text{C}_{\text{TC}}$
316 HCl vs. wind speed). Concentrations of CC were also positively correlated with wind speed ($r = 0.48$, **Fig.**
317 **S10**), indicating that wind has an effect on this aerosol component. Therefore, we compared the $\delta^{13}\text{C}$ time
318 series with average wind speeds and prevailing AMBT, from the HYSPLIT model (see colored bars in **Fig.**
319 **7**), which were divided into six regions as shown in **Fig. 1**.

320 The large differences in $\delta^{13}\text{C}$ values (or relatively more positive $\delta^{13}\text{C}_{\text{TC}}$ values) can be divided into three
321 categories. The most frequent differences were observed during periods of stronger winds (average WS
322 above 4 m s^{-1}) associated with the prevailing back trajectories from the North Canada region. These episodes
323 can be found mainly in summer and autumn 2016 and summer 2017. Such conditions favor dust
324 resuspension, which may also contain limestone, known to be abundant in this region (Not and Hillaire-
325 Marcel, 2012; Phillips and Grantz, 2001). The presence of a peak in soil dust carbonates in late
326 summer/early autumn is consistent with multidecadal aerosol aluminum observations at Alert (Sharma et
327 al., 2019; Sirois and Barrie, 1999). These observations also indicate a peak in soil dust aerosol in the spring
328 month of May (Sharma et al. 2019).

329 Second, in late February/March 2018, we observed significant enrichment of ^{13}C , which may probably be
330 linked to long range transport (LRT) from/over Europe, Greenland and North America (Fig. 6). Sources of
331 carbonate in this case may be, for example, calcifying marine phytoplankton (Monteiro et al., 2016), which
332 are abundant in the North Atlantic (Okada and Honjo, 1973). Another possibility is the volcanic and
333 subarctic semi-desert areas in Iceland (Arnalds et al., 2016).

334

Deleted: s

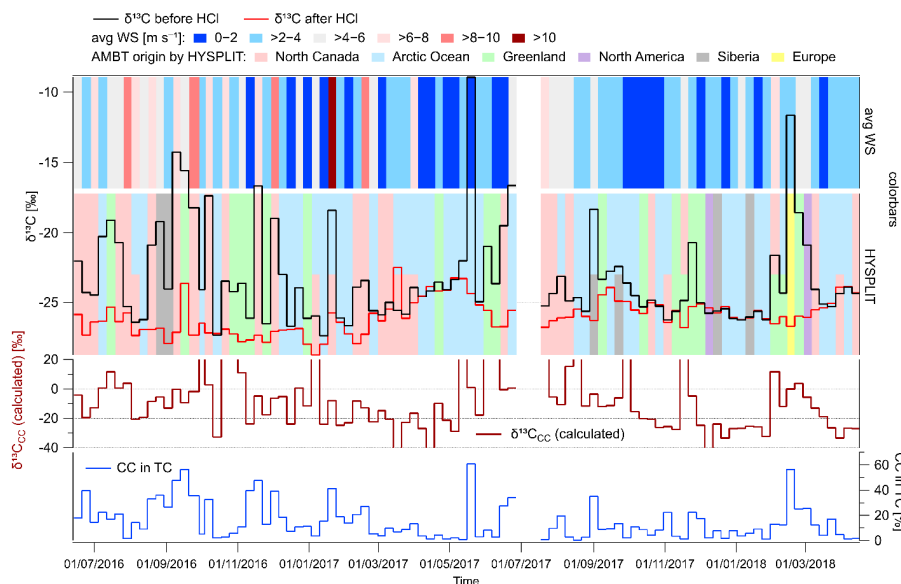
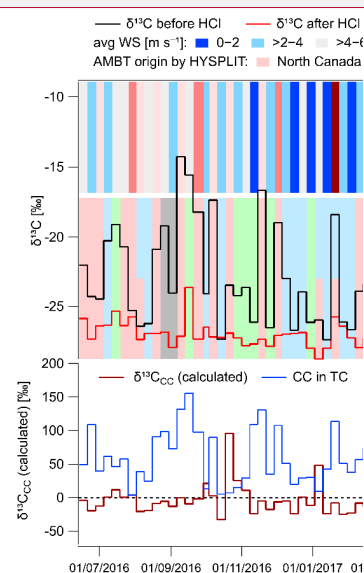


Figure 7. Time series of isotopic composition ($\delta^{13}C$) of TC before and after HCl treatment of samples (upper part) with color bars representing average wind speed (top) and origin of AMBT based on HYSPLIT model and divided to regions shown in Fig. 1 (middle part). Time series of the calculated $\delta^{13}C_{CC}$ (outliers less than -40 ‰ and more than +20 ‰ not depicted), and contribution of CC in TC (bottom).

The third case is a $\delta^{13}C$ difference observed during lower wind speeds coming from the Arctic Ocean or Greenland. This includes also the sample taken between 15-22 May 2017, whose thermograms are shown in Fig. 3, and which was most enriched in ^{13}C carbon. A recent study by Gu et al. (2023), which reports observations of summer carbonaceous aerosols in the Arctic Ocean, is relevant in this context. They also observed relatively more negative $\delta^{13}C$ values of TC, but in this case they did not consider the enriched ^{13}C carbon as a carbonate contribution, instead, they associated it with an input of fresh marine particulate organic carbon (MPOC) (Verwega et al., 2021). MPOC is formed by the conversion of inorganic carbon by marine phytoplankton through photosynthesis in ocean surface layer (Descolas-Gros and Fontugne, 1990), and this carbon can be partially released into the atmosphere as marine aerosol (Ceburnis et al., 2016). We cannot exclude the influence of MPOC on the TSP taken at the Alert station, but the specific EC/OC thermogram (Fig. 3, Fig. S2) shows rather an influence of $CaCO_3$. The presence of carbonates in surface seawater and their interference with organic coatings has been known for decades (Chave, 1965).



Deleted:

Deleted: together with

356 Dissolved CO₂ in the oceans consists mainly of inorganic substances, which are bicarbonates (HCO₃⁻;
357 >85%) and carbonates (ca 10%), and their content varies with temperature, pH, salinity and other
358 parameters (Zeebe, 2012). Carbonate, in the form of CaCO₃, is generally supersaturated in surface seawater
359 but its precipitation may be limited due to dissolved organic matter (Chave and Suess, 1970). In addition
360 to common inorganic reactions due to dissolved CO₂, the carbonate cycle is also influenced by marine life.
361 Phytoplankton such as coccolithophores (e.g. *Emiliania huxleyi*), could also contribute to formation of
362 carbonates (Smith et al., 2012). These organisms produce calcified shells called coccoliths, which are about
363 2–25 µm across (Monteiro et al., 2016). While these microfossils are mostly deposited on the seabed, they
364 are also likely to be released also into the atmosphere with marine aerosol from the upper sea layers. [Such](#)
365 [potential introduction of coccolith fragments by sea spray aerosol to the atmosphere is reported by](#)
366 [Mukherjee et al. \(2020\) for Arctic summer.](#) Whether through MPOC or inorganic carbon, this
367 phytoplankton influences the fractionation of ¹³C carbon (Holtz et al., 2017).

368 Coccolith microfossils contain enriched calcite with δ¹³C values around 0 ‰ (McClelland et al., 2017).
369 Limestone sediments in the Canadian Arctic are even more enriched, with δ¹³C values ranging from 2 to
370 8 ‰ (Beauchamp et al., 1987). After estimating δ¹³C_{CC} (see subsection 2.4), we observed that with a high
371 CC abundance in TC, the calculated δ¹³C_{CC} values are also seen around 0 ‰ (**Fig. 7** bottom, **Fig. S5**). This
372 suggests that when the TC contains a larger contribution of CC (suppose above 20%), it can be assumed
373 that a significant portion of the nominal CC is derived from limestone. However, the uncertainties in the
374 determining of δ¹³C_{CC}, mentioned in section 2.4, primarily due to the low CC contributions in TC, likely
375 prevent distinguishing whether the carbonates are from sediment resuspension or marine calcified shells.
376 Some insight, however, can be obtained from the AMBT analysis discussed earlier.

377 Finally, **Fig. 8a** confirms a strong dependence of δ¹³C_{TC} on the CC content in TC (r = 0.79). The dependence
378 of δ¹³C_{TC} directly on CC mass concentration is even stronger (r = 0.85, after excluding 1 outlier, **Fig. S11**).
379 Furthermore, we calculated the fractions of CC for individual samples via isotope mass balance (using a
380 δ¹³C of CC value of zero as the end member, see subsection 2.5.) and found that, overall, the calculated
381 results were approximately 5 ‰ lower than the measured CC/TC, with less scatter. In addition, we observed
382 an excellent correlation between δ¹³C of TC and the calculated fraction of CC, with r = 0.96 shown in **Fig.**
383 **8b**, indicating that more than 92 % of the variation in δ¹³C of TC can be explained by the dependency on
384 the fraction of CC.

385

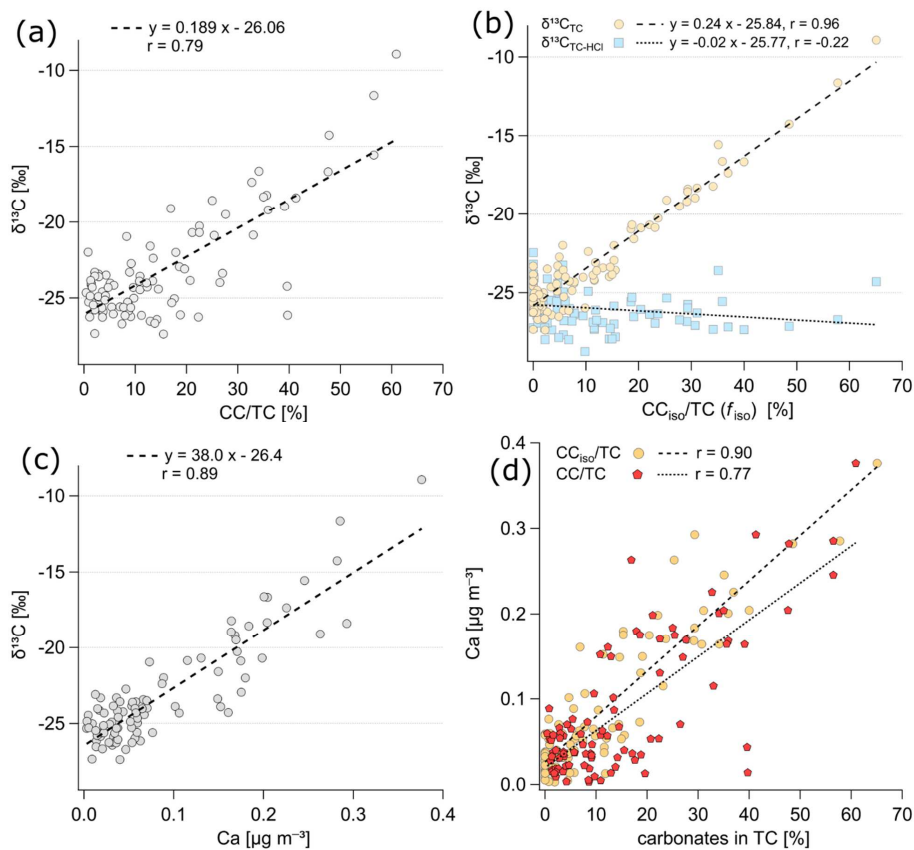


Figure 8. Dependence of (a) $\delta^{13}\text{C}_{\text{TC}}$ on the percentage contribution of CC in TC, (b) $\delta^{13}\text{C}_{\text{TC}}$ and $\delta^{13}\text{C}_{\text{TC-HCl}}$ on the calculated fraction of CC_{iso} in TC, (c) $\delta^{13}\text{C}_{\text{TC}}$ on Ca mass concentrations, and (d) Ca mass concentrations on percentage contribution of CC and CC_{iso} in TC.

Further support for the influence of $\delta^{13}\text{C}$ of TC in favor of carbonates is provided by its strong correlation with calcium ($r = 0.89$, **Fig. 8c**). Calcium is also strongly correlated with CC contribution in TC, with $r = 0.90$ for Ca vs. $\text{CC}_{\text{iso}}/\text{TC}$ (**Fig. 8d**). Apportionment of Ca amongst aerosol sources at Alert site (Sharma et al., 2019), using multidecadal observations and Positive Matrix Factorization analyses, showed that, on

average for both the period November to February, and March to May, Ca was associated 84 and 85% with windblown dust/soil and 12 and 8 % with sea salt aerosol, respectively.

We also investigated the possible contribution of carbon from magnesium carbonate. Magnesium was strongly correlated with sodium ($r = 0.91$, **Fig. S12**), indicating its link mainly to marine aerosol. In contrast, we observed no relationship between Mg and Ca; this dependence was strongly scattered (**Fig. S12**). Overall, the results indicate that the main contribution of CC, that strongly influences the $\delta^{13}\text{C}$ of TC, is mainly CaCO_3 . If there is a contribution of magnesium carbonate, it is rather episodic.

These results thus provide evidence that the CC content in aerosols, mostly of soil origin and to a lesser extent marine origin, strongly influences the $\delta^{13}\text{C}$ isotopic composition of TC in the Arctic atmosphere. Further research at different Arctic sites could reveal whether the non-negligible presence of CC in the TSP is the case only in the northern Canada region or a phenomenon observe in larger parts of Arctic.

4 Summary and conclusions

We found that the aerosol CC (i.e. carbonate carbon) fraction in Arctic TSP at Alert site is not negligible. The relative abundances of CC in TC ranged from 0 to 60 % with an average of 11 % over the entire measurement period. On average, 25 % (range: 0 to 81 %) of EC and 12% (range: 0 to 46 %) of OC was identified here as nominal CC. The influence of CC removal from the sample was also significantly reflected in the isotopic composition of $\delta^{13}\text{C}$ of TC. The effect of CC on $\delta^{13}\text{C}$ was particularly pronounced in the summer of 2016 and 2017, as well as during autumn 2016 due to strong local Arctic dust transport. In contrast, the effect of removing of CC on $\delta^{13}\text{C}$ was lowest in spring. Thus, CC content in TSP at Alert can sometimes strongly influence the $\delta^{13}\text{C}$ values of aerosols.

Based on the thermograms from EC/OC analyses and the calculated $\delta^{13}\text{C}_{\text{CC}}$, whose values were around 0 ‰ at high CC contributions to TC, we conclude that the major part of CC is derived from carbonates. Additionally, based on the isotope mass balance calculation (using 0 ‰ as $\delta^{13}\text{C}_{\text{CC}}$), an excellent dependency between $\delta^{13}\text{C}$ of TC and the calculated fraction of CC ($r = 0.96$) is observed, supporting that most of the variation of $\delta^{13}\text{C}$ of TC were due to the contribution of CC. Based on the AMBT analyses, we identified two possible carbonate sources. The first is eroded and resuspended limestone sediments in the northern Canadian region. The second source may be calcareous shells (coccoliths) produced by marine phytoplankton and transported from both the Arctic Ocean and the North Atlantic Ocean. However, the hypothesis of these sources requires further detailed research.

In general, when analysing $\delta^{13}\text{C}$ of TC in coarse aerosol or aerosols laden with dust, it must be taken into account that the resulting values may be strongly influenced by CC content. If CC is not removed prior to EC/OC analysis, CC may be mistakenly identified as EC during Improve_A analysis. This could, for example, affect modelling of the effect of carbonaceous aerosols on the Arctic climate, as EC (or black carbon) has a warming effect on the atmosphere, while CC has a lower warming effect.

Deleted: likely

Deleted: the opposite

Data availability. All relevant data for this paper are archived and are available upon request from the corresponding authors or online at repository here: <https://zenodo.org/records/14204515>

Supplementary data

Supplementary data to this article can be found as a pdf file uploaded together with this manuscript.

Author contribution. All authors contributed to the final version of this article. PV analyzed EC/OC before and after HCl treatment, as well as $\delta^{13}\text{C}$ of TC, AMBT analyses, evaluated all data and wrote the paper under the supervision of KK. BK analyzed $\delta^{13}\text{C}$ of TC after HCl treatment as well as supporting water soluble ions measurements. LH calculated contribution of CC_{iso} /TC based on $\delta^{13}\text{C}$ measurements. DD and MMH assisted in the gravimetry and other sample treatments. AP was responsible for the evaluation of Ca, Mg and Na data. SS provided meteorological data. SS with KK and LB managed the field campaign. All authors provided advice and feedback throughout the drafting and submission process.

Competing interests. Kimitaka Kawamura is an editor for Atmospheric Chemistry and Physics. The authors declare that they have no other conflict of interest.

Acknowledgements. This study was supported by JSPS grant no. 24221001, the JSPS Joint Research Program implemented in association with DFG (JSPS-LEAD with DFG: JPJSJRP 20181601) and from the Ministry of Education, Youth and Sports of the Czech Republic under project ACTRIS-CZ LM2023030. Authors thank the CFS Alert for maintaining the base, Andrew Platt Alert coordinator, the operator for ECCC and students for sample collection at Alert and shipment of these samples.

459

460 **Table 1:** Seasonal averages \pm standard deviations (medians in parentheses) of different variables in TSP at
 461 Alert site.

	Summer 2016	Autumn 2016	Winter 2016	Spring 2017	Summer 2017	Autumn 2017	Winter 2017	Spring 2018
N	12	13	13	13	10	13	13	6
OC [$\mu\text{g m}^{-3}$]	0.182 \pm 0.0 75 (0.177)	0.136 \pm 0.0 72 (0.106)	0.253 \pm 0.1 71 (0.237)	0.184 \pm 0.0 92 (0.151)	0.179 \pm 0.0 71 (0.155)	0.106 \pm 0.0 6 (0.128)	0.154 \pm 0.0 57 (0.177)	0.154 \pm 0.0 53 (0.153)
EC [$\mu\text{g m}^{-3}$]	0.037 \pm 0.0 21 (0.032)	0.056 \pm 0.0 55 (0.023)	0.100 \pm 0.1 21 (0.070)	0.057 \pm 0.0 37 (0.047)	0.031 \pm 0.0 15 (0.026)	0.019 \pm 0.0 13 (0.017)	0.055 \pm 0.0 36 (0.046)	0.032 \pm 0.0 18 (0.029)
TC [$\mu\text{g m}^{-3}$]	0.219 \pm 0.0 82 (0.216)	0.193 \pm 0.1 20 (0.126)	0.353 \pm 0.2 87 (0.290)	0.240 \pm 0.1 13 (0.186)	0.210 \pm 0.0 76 (0.186)	0.125 \pm 0.0 70 (0.146)	0.209 \pm 0.0 88 (0.225)	0.186 \pm 0.0 71 (0.182)
OC _{HCl} [$\mu\text{g m}^{-3}$]	0.150 \pm 0.0 67 (0.144)	0.103 \pm 0.0 52 (0.095)	0.215 \pm 0.1 25 (0.201)	0.172 \pm 0.0 88 (0.149)	0.159 \pm 0.0 62 (0.150)	0.096 \pm 0.0 51 (0.111)	0.140 \pm 0.0 52 (0.161)	0.146 \pm 0.0 56 (0.138)
EC _{HCl} [$\mu\text{g m}^{-3}$]	0.022 \pm 0.0 08 (0.022)	0.024 \pm 0.0 12 (0.021)	0.067 \pm 0.0 52 (0.058)	0.040 \pm 0.0 15 (0.040)	0.019 \pm 0.0 04 (0.019)	0.014 \pm 0.0 07 (0.015)	0.034 \pm 0.0 18 (0.031)	0.029 \pm 0.0 18 (0.024)
TC _{HCl} [$\mu\text{g m}^{-3}$]	0.172 \pm 0.0 70 (0.165)	0.127 \pm 0.0 61 (0.115)	0.282 \pm 0.1 75 (0.250)	0.211 \pm 0.1 01 (0.175)	0.178 \pm 0.0 64 (0.169)	0.110 \pm 0.0 57 (0.128)	0.174 \pm 0.0 68 (0.194)	0.175 \pm 0.0 74 (0.162)
CC [$\mu\text{g m}^{-3}$]	0.047 \pm 0.0 28 (0.052)	0.066 \pm 0.0 68 (0.030)	0.071 \pm 0.1 31 (0.034)	0.029 \pm 0.0 51 (0.010)	0.032 \pm 0.0 36 (0.020)	0.015 \pm 0.0 18 (0.006)	0.035 \pm 0.0 48 (0.014)	0.011 \pm 0.0 11 (0.007)
TC/mass [%]	10.3 \pm 3.8 (9.4)	6.0 \pm 1.9 (5.9)	7.8 \pm 3.5 (8.3)	5.9 \pm 2.4 (5.4)	13.2 \pm 5.4 (13.7)	8.3 \pm 6.2 (7.3)	6.0 \pm 1.6 (5.2)	7.8 \pm 1.8 (7.3)
CC/TC [%]	21.1 \pm 11.2 (19.5)	26.1 \pm 19.8 (32.7)	15.2 \pm 10.6 (13.8)	9.6 \pm 15.9 (4.3)	13.5 \pm 14.2 (6.2)	10.2 \pm 7.1 (8.9)	13.2 \pm 15.2 (8.0)	6.8 \pm 6.4 (4.4)
CC _{iso} /TC [%]	15.0 \pm 9.6 (14.9)	22.0 \pm 16.0 (15.6)	8.5 \pm 8.5 (6.7)	7.8 \pm 17.9 (1.2)	14.2 \pm 12.6 (9.8)	4.6 \pm 5.3 (4.4)	10.3 \pm 17.4 (0.2)	1.2 \pm 2.4 (0.0)
OC _{HCl} /TC [%]	68.3 \pm 12.5 (69.1)	59.0 \pm 18.1 (55.5)	65.6 \pm 9.5 (68.9)	72.5 \pm 13.9 (75.7)	76.5 \pm 12.8 (81.8)	77.7 \pm 6.3 (79.0)	71.0 \pm 13.4 (76.4)	78.5 \pm 4.6 (79.5)
EC _{HCl} /TC [%]	10.6 \pm 3.0 (10.5)	14.9 \pm 8.5 (12.7)	19.2 \pm 2.7 (20.2)	17.9 \pm 5.1 (16.5)	10.0 \pm 3.6 (9.3)	12.0 \pm 3.2 (11.6)	15.8 \pm 4.7 (15.8)	14.7 \pm 3.4 (13.3)
TC _{EA} [$\mu\text{g m}^{-3}$]	0.218 \pm 0.1 01 (0.214)	0.184 \pm 0.1 18 (0.120)	0.345 \pm 0.2 63 (0.287)	0.234 \pm 0.1 19 (0.200)	0.199 \pm 0.0 79 (0.174)	0.126 \pm 0.0 67 (0.124)	0.227 \pm 0.1 00 (0.224)	0.195 \pm 0.0 83 (0.191)
$\delta^{13}\text{C}_{\text{TC}}$ [‰]	-22.7 \pm 2.7 (-23.0)	-21.2 \pm 4.5 (-23.4)	-24.8 \pm 2.4 (-25.9)	-22.8 \pm 4.4 (-24.0)	-22.6 \pm 3.2 (-24.0)	-24.2 \pm 1.6 (-24.9)	-23.4 \pm 4.3 (-25.6)	-24.5 \pm 0.6 (-24.3)
TC _{EA-HCl} [$\mu\text{g m}^{-3}$]	0.141 \pm 0.0 63 (0.136)	0.092 \pm 0.0 52 (0.079)	0.273 \pm 0.1 96 (0.253)	0.199 \pm 0.1 08 (0.169)	0.157 \pm 0.0 65 (0.144)	0.103 \pm 0.0 52 (0.099)	0.173 \pm 0.0 68 (0.188)	0.184 \pm 0.0 80 (0.166)
$\delta^{13}\text{C}_{\text{TC-HCl}}$ [‰]	-26.6 \pm 0.7 (-26.6)	-27.0 \pm 1.1 (-27.2)	-27.1 \pm 0.9 (-27.0)	-24.4 \pm 1.1 (-24.3)	-26.2 \pm 0.5 (-26.2)	-25.3 \pm 0.8 (-25.2)	-26.0 \pm 0.4 (-26.1)	-24.7 \pm 0.8 (-24.7)
WS [m s^{-1}]	5.1 \pm 1.8 (4.5)	5.5 \pm 2.7 (5.6)	3.9 \pm 2.7 (3.1)	3.0 \pm 1.4 (3.5)	4.2 \pm 1.8 (4.6)	2.5 \pm 1.2 (2.1)	3.6 \pm 1.8 (3.4)	2.7 \pm 0.6 (2.6)
Temp. [°C]	5.0 \pm 4.6 (4.2)	-13.8 \pm 6.9 (-14.0)	-28.7 \pm 4.0 (-27.6)	-20.5 \pm 8.4 (-21.3)	1.2 \pm 4.6 (1.5)	-18.6 \pm 6.8 (-19.6)	-26.2 \pm 3.9 (-25.5)	-30.0 \pm 3.5 (-30.8)

462

463 **References:**

- 464 Arnalds, O., Dagsson-Waldhauserova, P. and Olafsson, H.: The Icelandic volcanic aeolian environment: Processes
465 and impacts - A review, *Aeolian Res.*, 20, 176–195, doi:10.1016/j.aeolia.2016.01.004, 2016.
- 466 Barrie, L. A. and Barrie, M. J.: Chemical components of lower tropospheric aerosols in the high Arctic: Six years of
467 observations, *J. Atmos. Chem.*, 11(3), 211–226, doi:10.1007/BF00118349, 1990.
- 468 Baudin, F., Bouton, N., Wattripont, A. and Carrier, X.: Carbonates thermal decomposition kinetics and their
469 implications in using Rock-Eval® analysis for carbonates identification and quantification, *Sci. Technol. Energy*
470 *Transit.*, 78, doi:10.2516/stet/2023038, 2023.
- 471 Bauer, J. J., Yu, X.-Y., Cary, R., Laulainen, N. and Berkowitz, C.: Characterization of the sunset semi-continuous
472 carbon aerosol analyzer., *J. Air Waste Manag. Assoc.*, 59(7), 826–833, doi:10.3155/1047-3289.59.7.826, 2009.
- 473 Beauchamp, B., Oldershaw, A. E. and Krouse, H. R.: Upper carboniferous to upper permian ¹³C-enriched primary
474 carbonates in the sverdrup basin, Canadian arctic: Comparisons to coeval Western North American Ocean Margins,
475 *Chem. Geol. Isot. Geosci. Sect.*, 65(3–4), 391–413, doi:10.1016/0168-9622(87)90016-9, 1987.
- 476 Carslaw, K. S., Lee, L. A., Reddington, C. L., Pringle, K. J., Rap, A., Forster, P. M., Mann, G. W., Spracklen, D. V.,
477 Woodhouse, M. T., Regayre, L. A. and Pierce, J. R.: Large contribution of natural aerosols to uncertainty in indirect
478 forcing, *Nature*, 503(7474), 67–71, doi:10.1038/nature12674, 2013.
- 479 Cavalli, F., Viana, M., Yttri, K. E., Genberg, J. and Putaud, J.-P.: Toward a standardised thermal-optical protocol for
480 measuring atmospheric organic and elemental carbon: the EUSAAR protocol, *Atmos. Meas. Tech.*, 3(1), 79–89,
481 doi:10.5194/amt-3-79-2010, 2010.
- 482 Ceburnis, D., Masalaite, A., Ovadnevaite, J., Garbaras, A., Remeikis, V., Maenhaut, W., Claeys, M., Sciare, J.,
483 Baisnée, D. and O'Dowd, C. D.: Stable isotopes measurements reveal dual carbon pools contributing to organic
484 matter enrichment in marine aerosol, *Sci. Rep.*, 6(July), 1–6, doi:10.1038/srep36675, 2016.
- 485 Chave, K. E.: Carbonates: Association with organic matter in surface seawater, *Science* (80-.), 148(June), 1723–
486 1724, doi:doi:10.1126/science.148.3678.1723, 1965.
- 487 Chave, K. E. and Suess, E.: Calcium Carbonate Saturation in Seawater: Effects of Dissolved Organic Matter,
488 *Limnol. Oceanogr.*, 15(4), 633–637, doi:10.4319/lo.1970.15.4.0633, 1970.
- 489 Chen, B., Cui, X. and Wang, Y.: Regional prediction of carbon isotopes in soil carbonates for Asian dust source
490 tracer, *Atmos. Environ.*, 142, 1–8, doi:10.1016/j.atmosenv.2016.07.029, 2016.
- 491 Chen, P., Kang, S., Abdullaev, S. F., Safarov, M. S., Huang, J., Hu, Z., Tripathee, L. and Li, C.: Significant
492 influence of carbonates on determining organic carbon and black carbon: A case study in Tajikistan, central Asia,
493 *Environ. Sci. Technol.*, 55(5), 2839–2846, doi:10.1021/acs.est.0c05876, 2021.

494 Chow, J. C., Watson, J. G., Pritchett, L. C., Pierson, W. R., Frazier, C. A. and Purcell, R. G.: The dri thermal/optical
 495 reflectance carbon analysis system: description, evaluation and applications in U.S. Air quality studies, *Atmos.*
 496 *Environ.*, 27A(8), 1185–1201, 1993.

497 Chow, J. C., Watson, J. G., Chen, L.-W. A., Chang, M. C. O., Robinson, N. F., Trimble, D. and Kohl, S.: The
 498 IMPROVE_A temperature protocol for thermal/optical carbon analysis: maintaining consistency with a long-term
 499 database., *J. Air Waste Manage. Assoc.*, 57(9), 1014–1023, doi:10.3155/1047-3289.57.9.1014, 2007.

500 Descolas-Gros, C. and Fontugne, M.: Stable carbon isotope fractionation by marine phytoplankton during
 501 photosynthesis, *Plant. Cell Environ.*, 13(3), 207–218, doi:10.1111/j.1365-3040.1990.tb01305.x, 1990.

502 England, M. R., Eisenman, I., Lutsko, N. J. and Wagner, T. J. W.: The Recent Emergence of Arctic Amplification,
 503 *Geophys. Res. Lett.*, 48(15), 1–10, doi:10.1029/2021GL094086, 2021.

504 Feltracco, M., Barbaro, E., Spolaor, A., Vecchiato, M., Callegaro, A., Burgay, F., Vardè, M., Maffezzoli, N., Dallo,
 505 F., Scoto, F., Zangrando, R., Barbante, C. and Gambaro, A.: Year-round measurements of size-segregated low
 506 molecular weight organic acids in Arctic aerosol, *Sci. Total Environ.*, 763, 142954,
 507 doi:10.1016/j.scitotenv.2020.142954, 2021.

508 Flanner, M. G., Zender, C. S., Randerson, J. T. and Rasch, P. J.: Present-day climate forcing and response from
 509 black carbon in snow, *J. Geophys. Res.*, 112(D11), D11202, doi:10.1029/2006JD008003, 2007.

510 Friman, M., Aurela, M., Saarnio, K., Teinilä, K., Kesti, J., Harni, S. D., Saarikoski, S., Hyvärinen, A. and Timonen,
 511 H.: Long-term characterization of organic and elemental carbon at three different background areas in northern
 512 Europe, *Atmos. Environ.*, 310(February), doi:10.1016/j.atmosenv.2023.119953, 2023.

513 Gensch, I., Kiendler-Scharr, A. and Rudolph, J.: Isotope ratio studies of atmospheric organic compounds: Principles,
 514 methods, applications and potential, *Int. J. Mass Spectrom.*, 365–366, 206–221, doi:10.1016/j.ijms.2014.02.004,
 515 2014.

516 Groot Zwaafink, C. D., Grythe, H., Skov, H. and Stohl, A.: Substantial contribution of northern high-latitude
 517 sources to mineral dust in the Arctic, *J. Geophys. Res.*, 121(22), 13,678–13,697, doi:10.1002/2016JD025482, 2016.

518 Gu, W., Xie, Z., Wei, Z., Chen, A., Jiang, B., Yue, F. and Yu, X.: Marine Fresh Carbon Pool Dominates Summer
 519 Carbonaceous Aerosols Over Arctic Ocean, *J. Geophys. Res. Atmos.*, 128(8), doi:10.1029/2022JD037692, 2023.

520 Hasegawa, S.: Experimental Characterization of PM2.5 Organic Carbon by Using Carbon-fraction Profiles of
 521 Organic Materials, *Asian J. Atmos. Environ.*, 16(2), 2021128, doi:10.5572/ajae.2021.128, 2022.

522 Holtz, L. M., Wolf-Gladrow, D. and Thoms, S.: Stable carbon isotope signals in particulate organic and inorganic
 523 carbon of coccolithophores – A numerical model study for *Emiliana huxleyi*, *J. Theor. Biol.*, 420(January), 117–
 524 127, doi:10.1016/j.jtbi.2017.01.030, 2017.

525 Hu, Z., Kang, S., Xu, J., Zhang, C., Li, X., Yan, F., Zhang, Y., Chen, P. and Li, C.: Significant overestimation of

526 black carbon concentration caused by high organic carbon in aerosols of the Tibetan Plateau, *Atmos. Environ.*,
527 294(June 2022), 119486, doi:10.1016/j.atmosenv.2022.119486, 2023.

528 Huang, L., Brook, J. R., Zhang, W., Li, S. M., Graham, L., Ernst, D., Chivulescu, A. and Lu, G.: Stable isotope
529 measurements of carbon fractions (OC/EC) in airborne particulate: A new dimension for source characterization and
530 apportionment, *Atmos. Environ.*, 40(15), 2690–2705, doi:10.1016/j.atmosenv.2005.11.062, 2006.

531 Huang, L., Zhang, W., Santos, G. M., Rodríguez, B. T., Holden, S. R., Vetro, V. and Czimczik, C. I.: Application of
532 the ECT9 protocol for radiocarbon-based source apportionment of carbonaceous aerosols, *Atmos. Meas. Tech.*,
533 14(5), 3481–3500, doi:10.5194/amt-14-3481-2021, 2021.

534 Jankowski, N., Schmidl, C., Marr, I. L., Bauer, H. and Puxbaum, H.: Comparison of methods for the quantification
535 of carbonate carbon in atmospheric PM10 aerosol samples, *Atmos. Environ.*, 42(34), 8055–8064,
536 doi:10.1016/j.atmosenv.2008.06.012, 2008.

537 Karanasiou, A., Diapouli, E., Cavalli, F., Eleftheriadis, K., Viana, M., Alastuey, A., Querol, X. and Reche, C.: On
538 the quantification of atmospheric carbonate carbon by thermal/optical analysis protocols, *Atmos. Meas. Tech.*, 4,
539 2409–2419, doi:10.5194/amt-4-2409-2011, 2011.

540 Kawai, K., Matsui, H. and Tobo, Y.: Dominant Role of Arctic Dust With High Ice Nucleating Ability in the Arctic
541 Lower Troposphere, *Geophys. Res. Lett.*, 50(8), 1–10, doi:10.1029/2022GL102470, 2023.

542 Kawamura, K. and Watanabe, T.: Determination of stable carbon isotopic compositions of low molecular weight
543 dicarboxylic acids and ketocarboxylic acids in atmospheric aerosol and snow samples, *Anal. Chem.*, 76(19), 5762–
544 5768, doi:10.1021/ac049491m, 2004.

545 Kawamura, K., Yanase, A., Eguchi, T., Mikami, T. and Barrie, L. A.: Enhanced atmospheric transport of soil
546 derived organic matter in spring over the Arctic, *Geophys. Res. Lett.*, 23(25), 3735–3738, doi:10.1029/96GL03537,
547 1996.

548 Laskin, A., Laskin, J. and Nizkorodov, S. A.: Chemistry of Atmospheric Brown Carbon, *Chem. Rev.*, 115(10),
549 4335–4382, doi:10.1021/cr5006167, 2015.

550 Liu, D., He, C., Schwarz, J. P. and Wang, X.: Lifecycle of light-absorbing carbonaceous aerosols in the atmosphere,
551 *npj Clim. Atmos. Sci.*, 3(1), doi:10.1038/s41612-020-00145-8, 2020.

552 Mbengue, S., Zikova, N., Schwarz, J., Vodička, P., Šmejkalová, A. H. and Holoubek, I.: Mass absorption cross-
553 section and absorption enhancement from long term black and elemental carbon measurements: A rural background
554 station in Central Europe, *Sci. Total Environ.*, 794, doi:10.1016/j.scitotenv.2021.148365, 2021.

555 McClelland, H. L. O., Bruggeman, J., Hermoso, M. and Rickaby, R. E. M.: The origin of carbon isotope vital effects
556 in coccolith calcite, *Nat. Commun.*, 8(May 2016), 1–16, doi:10.1038/ncomms14511, 2017.

557 Meinander, O., Dagsson-Waldhauserova, P., Amosov, P., Aseyeva, E., Atkins, C., Baklanov, A., Baldo, C., Barr, S.

558 L., Barzycka, B., Benning, L. G., Cvetkovic, B., Enchilik, P., Frolov, D., Gassó, S., Kandler, K., Kasimov, N.,
 559 Kavan, J., King, J., Koroleva, T., Krupskaya, V., Kulmala, M., Kusiak, M., Lappalainen, H. K., Laska, M., Lasne, J.,
 560 Lewandowski, M., Luks, B., Mcquaid, J. B., Moroni, B., Murray, B., Möhler, O., Nawrot, A., Nickovic, S., O'Neill,
 561 N. T., Pejanovic, G., Popovicheva, O., Ranjbar, K., Romanias, M., Samonova, O., Sanchez-Marroquin, A.,
 562 Schepanski, K., Semenov, I., Sharapova, A., Shevnina, E., Shi, Z., Sofiev, M., Thevenet, F., Thorsteinsson, T.,
 563 Timofeev, M., Umo, N. S., Uppstu, A., Urupina, D., Varga, G., Werner, T., Arnalds, O. and Vukovic Vimic, A.:
 564 Newly identified climatically and environmentally significant high-latitude dust sources, *Atmos. Chem. Phys.*,
 565 22(17), 11889–11930, doi:10.5194/acp-22-11889-2022, 2022.

566 Monteiro, F. M., Bach, L. T., Brownlee, C., Bown, P., Rickaby, R. E. M., Poulton, A. J., Tyrrell, T., Beaufort, L.,
 567 Dutkiewicz, S., Gibbs, S., Gutowska, M. A., Lee, R., Riebesell, U., Young, J. and Ridgwell, A.: Why marine
 568 phytoplankton calcify, *Sci. Adv.*, 2(7), 1–14, doi:10.1126/sciadv.1501822, 2016.

569 Moschos, V., Dzepina, K., Bhattu, D., Lamkaddam, H., Casotto, R., Daellenbach, K. R., Canonaco, F., Rai, P., Aas,
 570 W., Becagli, S., Calzolari, G., Eleftheriadis, K., Moffett, C. E., Schnelle-Kreis, J., Severi, M., Sharma, S., Skov, H.,
 571 Vestenius, M., Zhang, W., Hakola, H., Hellén, H., Huang, L., Jaffrezo, J. L., Massling, A., Nøjgaard, J. K., Petäjä,
 572 T., Popovicheva, O., Sheesley, R. J., Traversi, R., Yttri, K. E., Schmale, J., Prévôt, A. S. H., Baltensperger, U. and
 573 El Haddad, I.: Equal abundance of summertime natural and wintertime anthropogenic Arctic organic aerosols, *Nat.*
 574 *Geosci.*, doi:10.1038/s41561-021-00891-1, 2022.

575 Mukherjee, P., Reinfelder, J. R. and Gao, Y.: Enrichment of calcium in sea spray aerosol in the Arctic summer
 576 atmosphere, *Mar. Chem.*, 227(May 2019), 103898, doi:10.1016/j.marchem.2020.103898, 2020.

577 Muller, A., Lamb, E. G. and Siciliano, S. D.: The silent carbon pool: Cryoturbic enriched organic matter in Canadian
 578 High Arctic semi-deserts, *Geoderma*, 415(September 2021), 115781, doi:10.1016/j.geoderma.2022.115781, 2022.

579 Narukawa, M., Kawamura, K., Li, S.-M. and Bottenheim, J. W.: Stable carbon isotopic ratios and ionic composition
 580 of the high-Arctic aerosols: An increase in $\delta^{13}\text{C}$ values from winter to spring, *J. Geophys. Res.*, 113(D2), D02312,
 581 doi:10.1029/2007JD008755, 2008.

582 Not, C. and Hillaire-Marcel, C.: Enhanced sea-ice export from the Arctic during the Younger Dryas, *Nat. Commun.*,
 583 3(April 2014), 645–647, doi:10.1038/ncomms1658, 2012.

584 Okada, H. and Honjo, S.: Distribution of Oceanic Coccolithophorids in the Pacific., *Deep Sea Res.*, 20(4), 355–374,
 585 doi:10.1016/0011-7471(73)90059-4, 1973.

586 Petit, J. E., Favez, O., Albinet, A. and Canonaco, F.: A user-friendly tool for comprehensive evaluation of the
 587 geographical origins of atmospheric pollution: Wind and trajectory analyses, *Environ. Model. Softw.*, 88, 183–187,
 588 doi:10.1016/j.envsoft.2016.11.022, 2017.

589 Petzold, A., Ogren, J. A., Fiebig, M., Laj, P., Li, S. M., Baltensperger, U., Holzer-Popp, T., Kinne, S., Pappalardo,
 590 G., Sugimoto, N., Wehrli, C., Wiedensohler, A. and Zhang, X. Y.: Recommendations for reporting black carbon

591 measurements, *Atmos. Chem. Phys.*, 13(16), 8365–8379, doi:10.5194/acp-13-8365-2013, 2013.

592 Phillips, R. L. and Grantz, A.: Regional variations in provenance and abundance of ice-rafted clasts in Arctic Ocean
593 sediments: Implications for the configuration of late Quaternary oceanic and atmospheric circulation in the Arctic,
594 *Mar. Geol.*, 172(1–2), 91–115, doi:10.1016/S0025-3227(00)00101-8, 2001.

595 Pushkareva, E., Johansen, J. R. and Elster, J.: A review of the ecology, ecophysiology and biodiversity of
596 microalgae in Arctic soil crusts, *Polar Biol.*, 39(12), 2227–2240, doi:10.1007/s00300-016-1902-5, 2016.

597 Raman, R. S., Ramachandran, S. and Kedia, S.: A methodology to estimate source-specific aerosol radiative forcing,
598 *J. Aerosol Sci.*, 42(5), 305–320, doi:10.1016/j.jaerosci.2011.01.008, 2011.

599 Rodríguez, B. T., Huang, L., Santos, G. M., Zhang, W., Vetro, V., Xu, X., Kim, S. and Czimczik, C. I.: Seasonal
600 Cycle of Isotope-Based Source Apportionment of Elemental Carbon in Airborne Particulate Matter and Snow at
601 Alert, Canada, *J. Geophys. Res. Atmos.*, 125(23), 1–15, doi:10.1029/2020JD033125, 2020.

602 Savadkoobi, M., Pandolfi, M., Favez, O., Putaud, J. P., Eleftheriadis, K., Fiebig, M., Hopke, P. K., Laj, P.,
603 Wiedensohler, A., Alados-Arboledas, L., Bastian, S., Chazean, B., María, Á. C., Colombi, C., Costabile, F., Green,
604 D. C., Hueglin, C., Liakakou, E., Luoma, K., Listrani, S., Mihalopoulos, N., Marchand, N., Močnik, G., Niemi, J.,
605 V., Ondráček, J., Petit, J. E., Rattigan, O. V., Reche, C., Timonen, H., Titos, G., Tremper, A. H., Vratolis, S.,
606 Vodička, P., Funes, E. Y., Zíková, N., Harrison, R. M., Petäjä, T., Alastuey, A. and Querol, X.: Recommendations
607 for reporting equivalent black carbon (eBC) mass concentrations based on long-term pan-European in-situ
608 observations, *Environ. Int.*, 185(December 2023), 108553, doi:10.1016/j.envint.2024.108553, 2024.

609 Sharma, S., Lavoué, D., Chachier, H., Barrie, L. A. and Gong, S. L.: Long-term trends of the black carbon
610 concentrations in the Canadian Arctic, *J. Geophys. Res. D Atmos.*, 109(15), 1–10, doi:10.1029/2003JD004331,
611 2004.

612 Sharma, S., Leaitch, W. R., Huang, L., Veber, D., Kolonjari, F., Zhang, W., Hanna, S. J., Bertram, A. K. and Ogren,
613 J. A.: An evaluation of three methods for measuring black carbon in Alert, Canada, *Atmos. Chem. Phys.*, 17(24),
614 15225–15243, doi:10.5194/acp-17-15225-2017, 2017.

615 Sharma, S., Barrie, L. A., Magnusson, E., Brattström, G., Leaitch, W. R., Steffen, A. and Landsberger, S.: A Factor
616 and Trends Analysis of Multidecadal Lower Tropospheric Observations of Arctic Aerosol Composition, Black
617 Carbon, Ozone, and Mercury at Alert, Canada, *J. Geophys. Res. Atmos.*, 124(24), 14133–14161,
618 doi:10.1029/2019JD030844, 2019.

619 Sirois, A. and Barrie, L. A.: Arctic lower tropospheric aerosol trends and composition at Alert, Canada: 1980-1995,
620 *J. Geophys. Res.*, 104(D9), 11599–11618, 1999.

621 Smith, H. E. K., Tyrrell, T., Charalampopoulou, A., Dumousseaud, C., Legge, O. J., Birchenough, S., Pettit, L. R.,
622 Garley, R., Hartman, S. E., Hartman, M. C., Sagoo, N., Daniels, C. J., Achterberg, E. P. and Hydes, D. J.:
623 Predominance of heavily calcified coccolithophores at low CaCO₃ saturation during winter in the Bay of Biscay,

624 Proc. Natl. Acad. Sci. U. S. A., 109(23), 8845–8849, doi:10.1073/pnas.1117508109, 2012.

625 Stein, A. F., Draxler, R. R., Rolph, G. D., Stunder, B. J. B., Cohen, M. D. and Ngan, F.: NOAA’s HYSPLIT
626 atmospheric transport and dispersion modeling system, Bull. Am. Meteorol. Soc., 96(12), 2059–2077,
627 doi:10.1175/BAMS-D-14-00110.1, 2015.

628 Stein, R., Grobe, H. and Wahsner, M.: Organic carbon, carbonate, and clay mineral distributions in eastern central
629 Arctic Ocean surface sediments, Mar. Geol., 119(3–4), 269–285, doi:10.1016/0025-3227(94)90185-6, 1994.

630 Stjern, C. W., Samset, B. H., Myhre, G., Bian, H., Chin, M., Davila, Y., Dentener, F., Emmons, L., Flemming, J.,
631 Haslerud, A. S., Henze, D., Jonson, J. E., Kucsera, T., Lund, M. T., Schulz, M., Sudo, K., Takemura, T. and Tilmes,
632 S.: Global and regional radiative forcing from 20 % reductions in BC, OC and SO₄ - An HTAP2 multi-model study,
633 Atmos. Chem. Phys., 16(21), 13579–13599, doi:10.5194/acp-16-13579-2016, 2016.

634 Toom-Sauntry, D. and Barrie, L. A.: Chemical composition of snowfall in the high Arctic: 1990-1994, Atmos.
635 Environ., 36(15–16), 2683–2693, doi:10.1016/S1352-2310(02)00115-2, 2002.

636 Verwega, M. T., Somes, C. J., Schartau, M., Tuerena, R. E., Lorrain, A., Oeschles, A. and Slawig, T.: Description of
637 a global marine particulate organic carbon-13 isotope data set, Earth Syst. Sci. Data, 13(10), 4861–4880,
638 doi:10.5194/essd-13-4861-2021, 2021.

639 Vodička, P., Kawamura, K., Schwarz, J. and Ždímal, V.: Seasonal changes in stable carbon isotopic composition in
640 the bulk aerosol and gas phases at a suburban site in Prague, Sci. Total Environ., 803, 149767,
641 doi:10.1016/j.scitotenv.2021.149767, 2022.

642 Wang, H. and Kawamura, K.: Stable carbon isotopic composition of low-molecular-weight dicarboxylic acids and
643 ketoacids in remote marine aerosols, J. Geophys. Res. Atmos., 111(7), doi:10.1029/2005JD006466, 2006.

644 Winiger, P., Barrett, T. E., Sheesley, R. J., Huang, L., Sharma, S., Barrie, L. A., Yttri, K. E., Evangeliou, N.,
645 Eckhardt, S., Stohl, A., Klimont, Z., Heyes, C., Semiletov, I. P., Dudarev, O. V., Charkin, A., Shakhova, N.,
646 Holmstrand, H., Andersson, A. and Gustafsson: Source apportionment of circum-Arctic atmospheric black carbon
647 from isotopes and modeling, Sci. Adv., 5(2), 1–10, doi:10.1126/sciadv.aau8052, 2019.

648 Zeebe, R. E.: History of seawater carbonate chemistry, atmospheric CO₂, and ocean acidification, Annu. Rev. Earth
649 Planet. Sci., 40, 141–165, doi:10.1146/annurev-earth-042711-105521, 2012.

650